A microporous metal–organic framework constructed from a 1D column made of linear trinuclear manganese secondary building units†

Sehyun Jeong,[a] Jungwook Choi,[a] Mira Park,[a] Minhak Oh,[b] Dohyun Moon*[c] and Myoung Soo Lah*[b]

Received 5th January 2010, Accepted 29th January 2010
First published as an Advance Article on the web 8th March 2010
DOI: 10.1039/b927590h

A metal–organic framework (MOF) was prepared based on a 1D column made of a linear trinuclear manganese cluster as a secondary building unit (SBU), where the SBU is connected to two adjacent SBUs by carboxylates to form a 1D column and the column is further connected to four adjacent 1D columns *via* the SBUs to form a microporous MOF of pcu network topology.

Introduction

Porous metal–organic frameworks (MOFs) have great potentials in various applications such as gas storage,[1] separation,[2] and catalysis.[3] In particular, MOFs having potential exposed metal sites are attractive to many researchers because the open metal sites could be used for the enhancement of the hydrogen affinity[4] and used as active sites for various catalyses.[5] However, a rational design of a new porous MOF with potential exposed metal sites is still a challenge. Approaches using secondary building units (SBUs) have been proved to be very effective not only for the construction of new porous MOFs[6] but also for the generation of potential exposed metal sites in the pores of the MOFs.[5] It is well known that the reaction of manganese ions with carboxylate ligands often leads to a linear trinuclear manganese cluster with some ligated solvent molecules.[7] When the trinuclear cluster with ligated solvent molecules is utilized as an SBU in the construction of porous MOFs, the SBU with the ligated solvent molecules could be utilized for the generation of the exposed metal sites in the porous MOFs.

Here, we report on the preparation and characterization of a microporous 3D MOF with potential exposed metal sites. It is based on a 1D column made of trinuclear manganese clusters as SBUs by using a manganese(II) ion as a metal source and 2,7-naphthalene dicarboxylic acid (2,7-H_2ndc) as a rigid bent dicarboxylate, where *N*,*N*′-dimethylformamide (DMF) solvent molecules are ligated to the metal center of the trinuclear manganese SBUs.

Experimental

General procedures

All other reagents were purchased from commercial sources and were used without further purification. Elemental analyses were conducted at the Elemental Analysis Laboratory of the Korean Basic Science Institute, Korea. FT–IR spectra were recorded as KBr pellets with a Varian 1000 FT–IR spectrophotometer (4000–400 cm^{-1}). Powder X-ray diffraction (PXRD) data was recorded using a Rigaku D/M 2200T automated diffractometer at room temperature with a step size of 0.02° in 2θ angle. The variable-temperature PXRD (VT-PXRD) measurements were carried using a Bruker D8 Advance system out in the air, and the sample was heated gradually from room temperature with a holding time of at least 30 min at each temperature. Simulated PXRD patterns were calculated with the Material Studio program[8] using the single crystal data.

Low-pressure gas sorption measurements

The nitrogen sorption isotherms were measured with a BEL-SORP-mini II (BEL Japan, Inc.) in a standard volumetric technique, at 77 K. The sorption of hydrogen was measured using liquid nitrogen (77 K) or liquid argon (87 K) as coolant. The sorption of carbon dioxide and methane was carried out in a mixture of dry ice and isopropanol (195 K). The gases used were of extra-pure quality (N50 for nitrogen and N60 for hydrogen). A part of the N_2 sorption isotherms in the P/P_0 range 0.010–0.091 was fitted to the Brunauer–Emmett–Teller (BET) equation to determine the BET surface areas. For the Langmuir surface areas, data from the whole adsorption isotherm were used.

Synthesis

$[Mn_3(2,7\text{-ndc})_3(DMF)_2]\cdot DMF\cdot 1.5H_2O$ ($1\cdot DMF\cdot 1.5H_2O$). A 0.0541 g (0.250 mmol) sample of 2,7-H_2ndc (Amfinecom Inc., 97.5%) was dissolved in 5 mL of DMF in a 10 mL vial. To the above solution was added a 0.0495 g (0.250 mmol) sample of manganese(II) acetate tetrahydrate. The vial was sealed and heated to 120 °C for 5 days, after which was cooled to room temperature. Pale brown block-shaped crystals were obtained. These were filtered and then air-dried. Yield 0.0151 g (17.5%). IR spectrum (KBr, cm^{-1}): 3411(s), 1675(sh), 1654(s), 1636(m), 1591(m), 1535(s), 1508(m), 1440(s), 1396(s), 1361(s), 1258(w), 1239(w), 1201(w), 1153(w), 1142(w), 1106(w), 1062(w), 958(w), 937(w), 865(w), 840(w), 829(w), 796(m), 761(w), 668(w), 649(w), 607(m), 575(w), 504(w), 472(w), 433(w), 406(w). Elemental

[a]*Department of Chemistry and Applied Chemistry, Hanyang University, Ansan, Kyunggi-do, 426-791, Korea*
[b]*Interdisciplinary School of Green Energy, Ulsan National Institute of Science and Technology, Ulsan, 689-805, Korea. E-mail: mslah@hanyang.ac.kr; Fax: +82 52 217 2909; Tel: +82 52 217 2931*
[c]*Beamline Division, Pohang Accelerator Laboratory, Pohang, Kyungbook 790-784, Korea. E-mail: dmoon@postech.ac.kr; Fax: +82 54 279 1599; Tel: +82 54 279 1547*

† Electronic supplementary information (ESI) available: Supplementary figures. CCDC reference number 750113. For ESI and crystallographic data in CIF or other electronic format see DOI: 10.1039/b927590h

analysis (EA) for $\mathbf{1}\cdot DMF\cdot 1.5H_2O$ ($Mn_3C_{45}H_{42}N_3O_{16.5}$), calculated: C 51.30, H 4.02, N 3.99%, found: C 51.77, H 4.17, N 4.17.

$[Mn_3(2,7\text{-ndc})_3(DMF)_{0.8}]\cdot 3.2H_2O$ ($\mathbf{1a}\cdot 3.2H_2O$). The as-synthesized sample, $\mathbf{1}\cdot DMF\cdot 1.5H_2O$, was transferred to fresh DMF solvent and held for 2–3 days. The activated sample, **1a**, was prepared by vacuum-drying the DMF-soaked sample at 180 °C for overnight, and then exposing to air. Yield 0.0132 g (16.3%). IR spectrum (KBr, cm^{-1}): 3402(s), 1655(s), 1636(m), 1608(m), 1592(m), 1530(s), 1507(m), 1439(s), 1397(s), 1361(s), 1263(w), 1238(w), 1201(w), 1145(w), 1100(w), 958(w), 934(w), 866(w), 849(w), 828(w), 796(m), 759(w), 666(w), 648(w), 622(w), 607(m), 566(w), 503(w), 471(w), 435(w), 401(w). EA for $\mathbf{1a}\cdot 3.2H_2O$ ($Mn_3C_{38.4}H_{30}N_{0.8}O_{16}$), calculated: C 49.94, H 3.27, N 1.21%, found: C 49.47, H 3.48, N 1.46%.

$[Mn_3(2,7\text{-ndc})_3(DMF)_{0.3}]\cdot H_2O$ ($\mathbf{1b}\cdot H_2O$). The activated sample, **1b**, was prepared the same as **1a**, but at 280 °C. IR spectrum (KBr, cm^{-1}): 3422(s), 1655(w), 1635(m), 1591(m), 1535(s), 1507(m), 1432(s), 1394(s), 1356(s), 1237(m), 1192(w), 1144(w), 957(w), 931(w), 859(w), 846(w), 796(m), 757(w), 669(w), 648(w), 608(w), 469(w), 413(w). EA for $\mathbf{1b}\cdot H_2O$ ($Mn_3C_{36.9}H_{22.1}N_{0.3}O_{13.3}$), calculated: C 52.31, H 2.63, N 0.50%, found: C 52.76, H 2.84, N 1.11%.

Crystallographic data collection and refinement of the structure

The diffraction data of a single crystal of **1** were measured at 99 K with synchrotron radiation ($\lambda = 0.80000$ Å) on a 4AMXW ADSC Quantum-210 detector with a Pt-coated Si double crystal monochromator at the Pohang Accelerator Laboratory (PAL), Korea. The ADSC Quantum-210 ADX program[9] was used for data collection, and HKL2000 (Ver. 0.98.698a)[10] was used for cell refinement, reduction and absorption correction.

Crystal structure determination for $[Mn_3(2,7\text{-ndc})_3(DMF)_2]\cdot 0.5DMF$, ($\mathbf{1}\cdot 0.5DMF$). Crystal data: $Mn_3C_{43.5}H_{35.5}N_{2.5}O_{14.5}$, fw = 990.06 g mol^{-1}, triclinic, space group $P\bar{1}$, $a = 12.283(3)$, $b = 13.386(3)$, $c = 13.931(3)$ Å, $\alpha = 102.14(3)°$, $\beta = 101.47(3)°$, $\gamma = 95.13(3)°$, $V = 2173.9(8)$ $Å^3$, $Z = 2$, μ(synchrotron, $\lambda = 0.80000$ Å) = 0.929 mm^{-1}, 19968 reflections were collected, and 10116 were unique [$R_{int} = 0.0507$]. The structure was solved by a direct method and refined by full-matrix least-squares calculations with the SHELXTL-PLUS software package.[11] Four manganese sites with two in the crystallographic inversion centers, three ligand units, two coordinating DMF molecules with one of them statistically disordered, and an additional disordered noncoordinating DMF on an inversion center were identified as the asymmetric unit. All nonhydrogen atoms were refined anisotropically; hydrogen atoms except those attached to noncoordination solvent molecules were assigned isotropic displacement coefficients U(H) = 1.2U(C) or 1.5U(C_{methyl}), and their coordinates were allowed to ride on their respective atoms. Solvent molecules of bad geometry were refined with geometry restraints during the least-squares refinement. The refinement converged to a final $R_1 = 0.0475$ and $wR_2 = 0.1295$ for 8244 reflections with $I > 2\sigma(I)$, $R_1 = 0.0592$ and $wR_2 = 0.1354$ for all 19968 reflections. The largest difference peak and hole were 0.670 and −0.800 e·$Å^{-3}$, respectively. A summary of the crystal and intensity data is given in Table 1. CCDC-750113 contains the supplementary crystallographic data.†

Table 1 Crystallographic data and structure refinement summary

	1
Chemical formula	$Mn_3C_{43.5}H_{35.5}N_{2.5}O_{14.5}$
Formula weight	990.06
Crystal system	Triclinic
Space group	$P\bar{1}$
T/K	99(2)
Wavelength (λ/Å)	0.80000
a/Å	12.283(3)
b/Å	13.386(3)
c/Å	13.931(3)
α (°)	102.14(3)
β (°)	101.47(3)
γ (°)	95.13(3)
V/$Å^3$	2173.9(8)
Z	2
D Mg^{-1} cm^{-3}	1.513
μ/mm^{-1}	0.929
$2\theta_{max}$ (°)	63.52
F(000)	1010
Reflns measured	19968
Obsd reflns	10116
R_{int}	0.0507
R^a/wR^b ($I > 2\sigma(I)$)	0.0475/0.1295

^{a} $R = \sum(|F_o| - |F_w|)/\sum|F_o|$. ^{b} $R_w = [\sum[w(F_o^2 - F_w^2)^2]/\sum w(F_o^2)^2]^{1/2}]$.

Results and discussion

A solvothermal reaction of manganese acetate tetrahydrate with 2,7-H_2ndc in DMF at 120 °C for 5 days led to a pale brown block-shaped crystalline product. A single crystal X-ray diffraction study revealed that the structure is a microporous 3D MOF based on carboxylate bridged 1D columns made of trinuclear

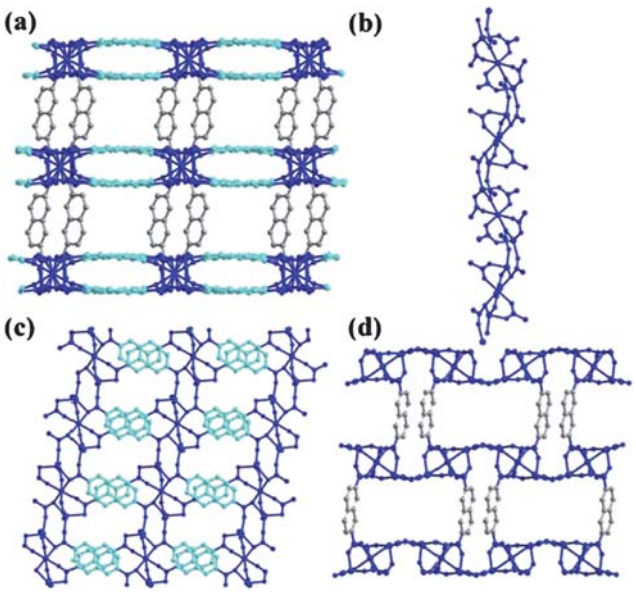

Fig. 1 (a) A 3D packing diagram viewed along [011] direction. (b) A 1D column viewed along [210] direction. Two 2D layers viewed along (c) [01–1] direction and (d) [211] direction, respectively. All solvent molecules including the ligated DMF molecules have been removed for clarity.

manganese clusters as SBUs, $[Mn_3(2,7\text{-ndc})_3(DMF)_2]$, **1** (Fig. 1). The 1D column consists of two different manganese centers bridged by two different types of carboxylate bridging modes (Fig. 1b). The first type is a tris-carboxylate bridging mode with a *syn-syn* bridging carboxylate, a *syn-anti* bridging carboxylate, and a μ^2-carboxylate, while the second type is a bis-carboxylate bridging mode with two *syn-anti* bridging carboxylates. A distorted octahedral manganese ion on a crystallographic inversion center involved in the tris-carboxylate bridging mode leads to a linear trinuclear manganese cluster as an SBU. The SBU is interconnected to the adjacent SBUs *via* the bis-carboxylate bridging mode, between the terminal manganese ions of the linear trinuclear clusters, to form a carboxylate bridged 1D column. The central manganese atom of the SBU has an octahedral coordination environment with six carboxylate oxygen atoms from six different ligands. The terminal manganese atoms of the SBU in a distorted trigonal bipyramidal coordination environment have four carboxylate oxygen atoms from four different ligands and one oxygen atom from a ligated DMF molecule at the fifth apical site of the metal geometry (Fig. 1b). The SBUs in the 1D column are further interconnected to the four SBUs in four adjacent 1D columns *via* the two different types of ligand bridging modes (Fig. 1c, 1d, and S1†). Each trinuclear SBU of the 1D column is doubly interconnected to the two SBUs of two adjacent 1D columns to form a 2D layer. The trinuclear SBU of the 1D column is further interconnected to two other SBUs of the other two adjacent 1D columns in an approximate perpendicular to the previous two adjacent 1D columns to form a 3D porous MOF based on a 1D column (Fig. 1a). The extensive π–π stacking interactions between the naphthyl rings (~3.4 Å inter-plane distance, Fig. 2) reinforce the structural rigidity of the framework. The MOF could be alternatively described as an MOF of a **pcu** network topology when the SBU is considered as a hexatopic octahedral node having three pairs of bridging modes between the SBUs (Fig. 3).[12] The 3D MOF, **1**, has 1D channels with a diameter of ~5 Å along the crystallographic [011] direction with the total

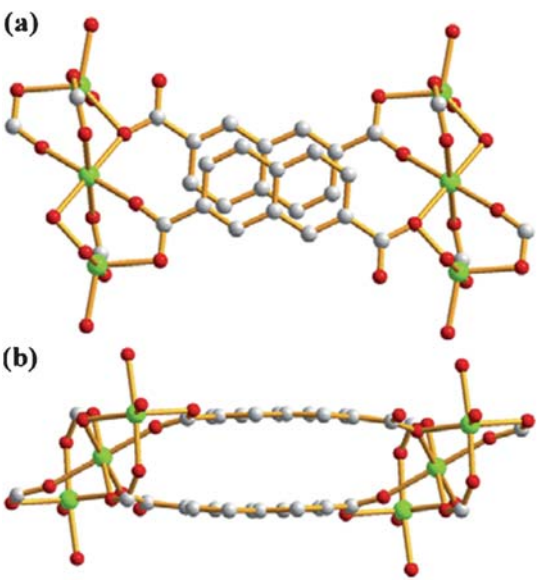

Fig. 2 π–π Stacking interactions between the naphthyl rings of the ligands.

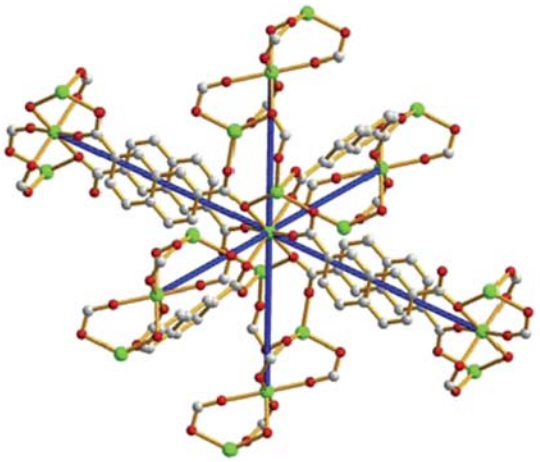

Fig. 3 The SBU comprising a linear trinuclear manganese cluster as a hexatopic octahedral node.

pore volume of 349 $Å^3$ per unit cell, which corresponds to 16.1% of the total crystal volume (Fig. S2†).

Thermogravimetric analysis (TGA) of the as-synthesized **1** revealed multistep weight loss before decomposition (Fig. 4a). The first two-step weight loss of about 2.2% and 6.8% occurred at temperatures of ~82 °C and ~165 °C, respectively. This corresponds to the loss of lattice solvent molecules, water, and DMF, in the solvent cavity (calc. 2.6% for one and a half H_2O molecules and 6.9% for a DMF molecule in the solvent cavity). The next two-step weight loss of about 6.4% and 5.6% occurred at temperature of ~220 °C and ~335 °C, respectively, which corresponds to the loss of two ligated DMF molecules (calc. 13.9% for two DMF molecules). The decomposition of **1** commenced at ~360 °C. The TGA of the activated **1a** revealed a two-step weight loss prior to decomposition (Fig. 4b). The first-step weight loss of about 6.3% occurred up to 120 °C, which corresponds to the loss of 3.2 water molecules reabsorbed into the solvent cavity (calc. 6.2% for 3.2 H_2O molecules in the solvent cavity). The second-step weight loss of about 6.5% occurred up to ~350 °C, which corresponds to the loss of 0.8 DMF molecule ligated at the metal center (calc. 6.3% for 0.8 DMF molecule). The decomposition of **1a** occurred at ~360 °C, as in the case of **1**. The TGA results match with the EA results of **1a** with 0.8 DMF and 3.2 water molecules per the trinuclear SBU. Although the single crystal X-ray analysis shows the presence of two ligated DMF per the SBU in **1**, the vacuum-drying overnight at 180 °C removes approximately one ligated DMF molecule per trinuclear SBU without significant structural transformation of the framework. The TGA of the activated **1b** also revealed a two-step weight loss prior to decomposition (Fig. 4c). The first-step weight loss of about 2.0% occurred up to 120 °C, which corresponds to the loss of a water molecule reabsorbed into the solvent cavity (calc. 2.1% for a water molecule in the solvent cavity). The second-step weight loss of about 2.5% occurred up to ~330 °C, which corresponds to the loss of 0.3 DMF molecule ligated at the metal center (calc. 2.6% for 0.3 DMF molecule). The decomposition of **1b** also occurred at ~360 °C, as in the case of **1** and **1a**.

The PXRD pattern of the bulk crystalline sample of the activated **1a** was similar to the simulated pattern of the single crystal structure of **1** (Fig. 5). The similarity of the PXRD pattern of

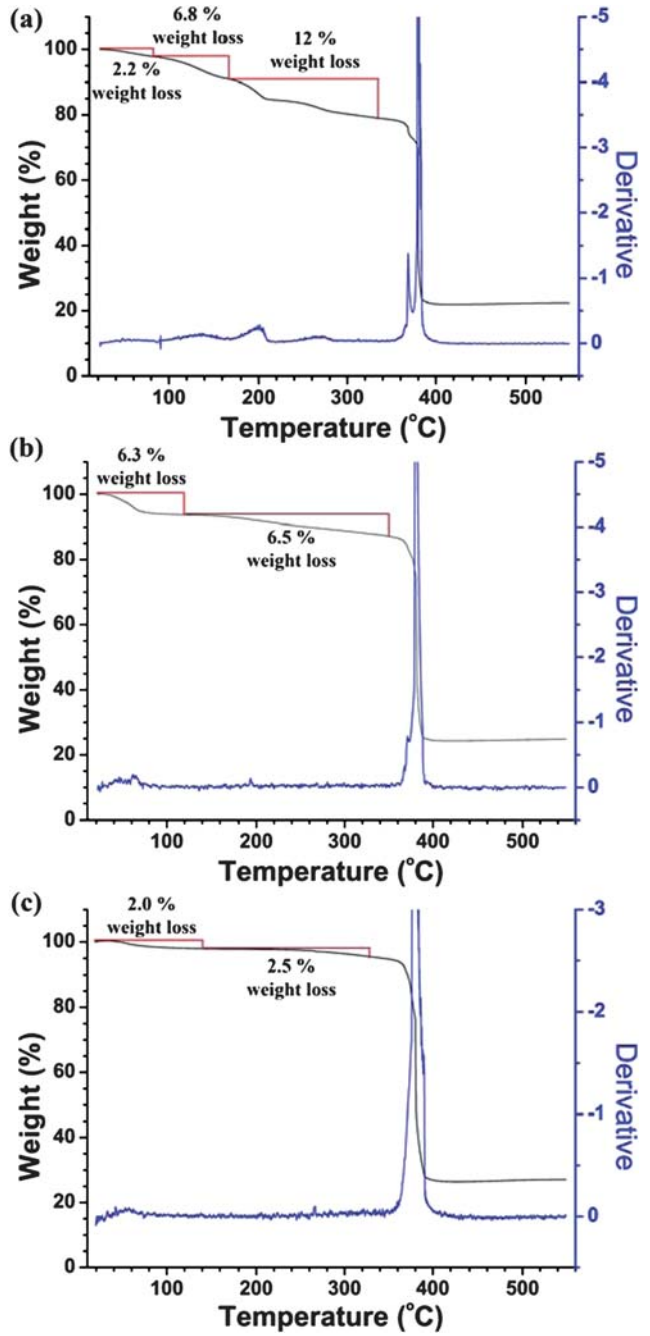

Fig. 4 TGA (a) as-synthesized sample, **1**. (b) activated at 180 °C, **1a**. (c) activated at 280 °C, **1b**.

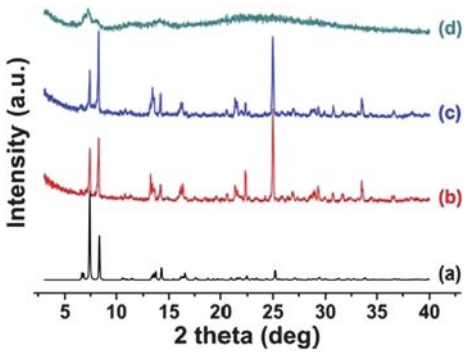

Fig. 5 PXRD patterns: (a) simulation from the single crystal structure of **1**, (b) as-synthesized, **1**, (c) activated at 180 °C, **1a**, and (d) activated at 280 °C, **1b**.

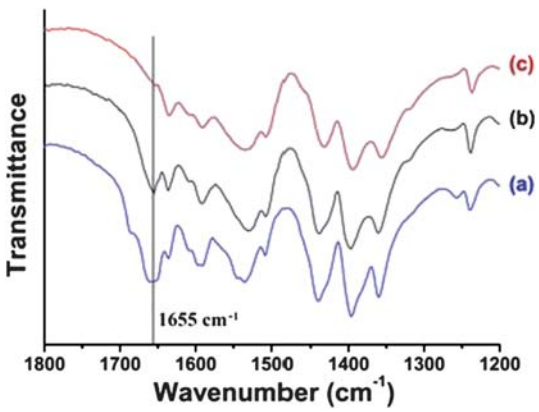

Fig. 6 IR spectra of (a) an as-synthesized sample, **1**, (b) a sample activated at 180 °C, **1a**, and (c) a sample activated at 280 °C, **1b**.

a sample vacuum-dried at 180 °C, the activated **1a**, to that of the as-synthesized bulk sample suggests that the guest solvent molecules including some of the ligated DMF molecules could be removed from the solvent cavity without significant disturbance of the framework structure. However, the PXRD pattern of a sample vacuum-dried at 280 °C, the activated **1b**, showed a significant loss of crystallinity. The removal of the most of the ligated solvent from the framework in **1b**, as confirmed by the IR spectrum (Fig. 6) and the TGA (Fig. 4c), may be responsible for such a change in the PXRD pattern. The overall thermal stability of the as-synthesized **1** was also demonstrated using variable temperature PXRD (Fig. 7). However, the variation in the peak positions and the intensity distribution, depending on temperatures, indicates that the structure is not static but dynamic. The shift of a major diffraction peak around ~7.5° in a 2θ angle to slightly higher diffraction angle could be interpreted as follows: solvent removal from the pores, including the ligated solvent molecules, leads to the shrinkage of the framework without complete destruction of the framework but with significant structural reorganization in the local structure of the framework.[13]

The N_2 sorption isotherm of **1a** at 77 K is a type I isotherm (Fig. 8), which indicated that **1a** has permanent micropores, as is expected from the single crystal structure of **1** and the PXRD of **1a**. The BET and Langmuir surface areas of **1a** were calculated to be 350 m^2g^{-1} and 450 m^2g^{-1}, respectively. The measured pore volume from the N_2 sorption, 0.158 cm^3g^{-1}, is slightly larger than the pore volume determined from the single crystal structure having two ligated DMF molecules per trinuclear manganese cluster (0.111 cm^3g^{-1}), which suggests that the MOF has lost some of its ligated DMF molecules during the activation process. Partial loss of the ligated DMF molecules is also in agreement with the TGA and EA results. However, the sample activated at 280 °C, **1b**, did not show any N_2 adsorption (Fig. 8). There was also no indication of adsorptions of other gas molecules such as

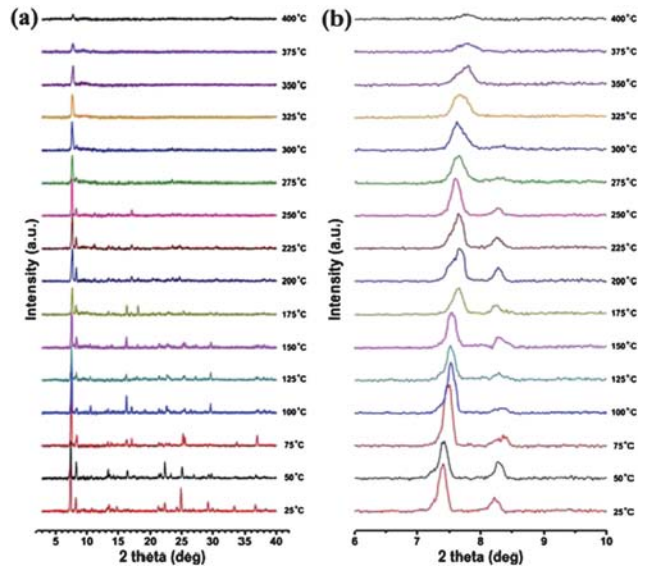

Fig. 7 (a) VT-PXRD patterns of an as-synthesized sample, **1**. (b) The expanded PXRD patterns for the low 2θ angle region.

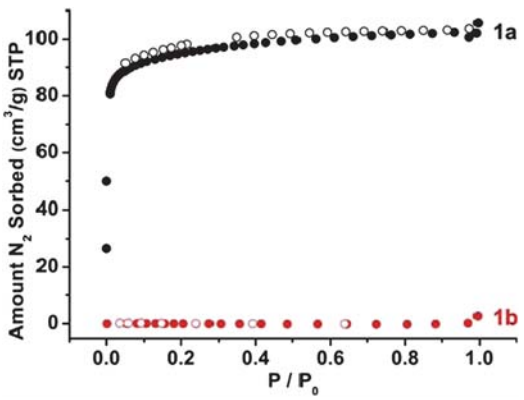

Fig. 8 N_2 sorption isotherms of **1a** and **1b** at 77 K (solid and open shapes represent adsorption and desorption, respectively).

H_2, CO_2, and CH_4 on **1b**. The removal of most of the ligated DMF molecules in the framework led to the collapse of the framework, with no accessible pores.

The H_2 sorption isotherm on **1a** was measured at 77 K and 87 K. The hydrogen uptakes were 84 cm^3g^{-1} (0.75 wt %) and 67 cm^3g^{-1} (0.60 wt %) at 1 atm, respectively (Fig. 9a). The H_2 storage capacity of **1a** was in the range expected from the BET or Langmuir surface area.[9a–b] The H_2 adsorption enthalpies calculated using a virial equation[14] ranged from 8.0 to 6.4 kJ mol^{-1} depending on the degree of H_2 loading (Fig. 9b). These high adsorption enthalpies of H_2 on **1a** might originate from the presence of exposed metal sites and the small pore diameter of the framework.

1a was also subjected to CO_2 and CH_4 sorption studies. At 195 K and 1 bar the adsorption amounts of CO_2 and CH_4 on **1a** were 78 g L^{-1} and 58 g L^{-1}, respectively (Fig. 10). The ratio of CO_2 *vs.* CH_4 uptake capacities on **1a**, ~1.3, is quite low compared with the usual values for other microporous MOFs.[15]

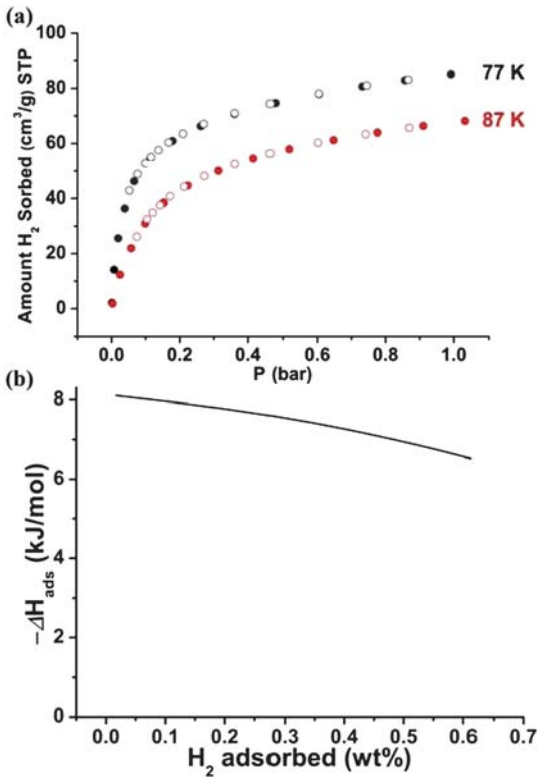

Fig. 9 (a) H_2 sorption isotherms on **1a** at 77 K (black) and 87 K (red), respectively (solid and open circles represent adsorption and desorption, respectively). (b) H_2 adsorption enthalpies on **1a**.

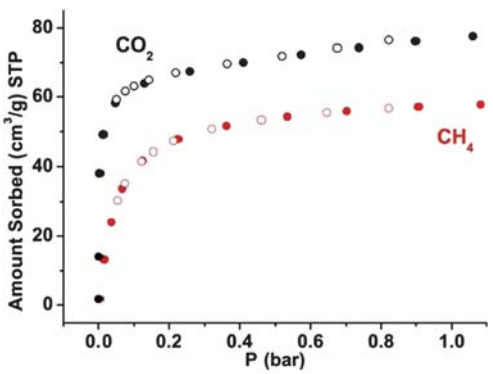

Fig. 10 Gas sorption isotherm of **1a** for CH_4 and CO_2 at 195 K (solid and open circles represent adsorption and desorption, respectively).

Conclusions

We could prepare a microporous 3D MOF based on a 1D column made of a trinuclear manganese cluster as an SBU. The SBU is connected to two adjacent SBUs by two chelating bidentate bridging μ^2-carboxylates, which leads to an infinite 1D columnar structure. The trinuclear manganese cluster in the 1D columnar structure acts as a four connecting node and the 1D columnar structure is further connected to four adjacent 1D columnar structures using 2,7-ndc to form a microporous 3D MOF of **pcu** network topology. When the solvent molecules in the cavity including some ligated ones were removed from the framework, the metal sites with reduced coordination numbers

could be generated within the 1D solvent cavity. The MOF with some exposed metal sites, **1a**, has permanent micropores; however, the MOF with no ligated solvent molecules does not show any permanent porosity. The exposed metal sites in the permanent pores of **1a** might play an important role in metal-ion assisted catalysis.

Acknowledgements

This work was supported by WCU program through the National Research Foundation of Korea. The authors also acknowledge PAL for beamline use (2009-3063-08).

References

1 (*a*) J.-E. Lee and J. Yun, *Angew. Chem., Int. Ed.*, 2008, **47**, 2; (*b*) D. Zhao, D. Yuan and H.-C. Zhou, *Energy Environ. Sci.*, 2008, **1**, 222; (*c*) J. L. C. Rowsell and O. M. Yaghi, *Angew. Chem., Int. Ed.*, 2005, **44**, 4670; (*d*) S. Ma, D. Sun, J. M. Simmons, C. D. Collier, D. Yuan and H.-C. Zhou, *J. Am. Chem. Soc.*, 2008, **130**, 1012; (*e*) A. R. Millward and O. M. Yaghi, *J. Am. Chem. Soc.*, 2005, **127**, 17998; (*f*) H. K. Chae, D. Y. Siberio-Perez, J. Kim, Y. B. Go, M. Eddaoudi, A. J. Matzger, M. O'Keeffe and O. M. Yaghi, *Nature*, 2004, **427**, 523; (*g*) R. Matsuda, R. Kitaura, S. Kitagawa, Y. Kubota, R. V. Belosludov, T. C. Kobayashi, H. Sakamoto, T. Chiba, M. Takata, Y. Kawazoe and Y. Mita, *Nature*, 2005, **436**, 238.

2 (*a*) J.-R. Li, R. J. Kuppler and H.-C. Zhou, *Chem. Soc. Rev.*, 2009, **38**, 1477; (*b*) S. Ma, D. Sun, X.-S. Wang and H.-C. Zhou, *Angew. Chem., Int. Ed.*, 2007, **46**, 2458; (*c*) D. N. Dybtsev, H. Chun, S. H. Yoon, D. Kim and K. Kim, *J. Am. Chem. Soc.*, 2004, **126**, 32; (*d*) L. Pan, B. Parker, X. Huang, D. H. Olson, J. Y. Lee and J. Li, *J. Am. Chem. Soc.*, 2006, **128**, 4180; (*e*) M. Dincă and J. R. Long, *J. Am. Chem. Soc.*, 2005, **127**, 9376.

3 (*a*) J. S. Seo, D. Whang, H. Lee, S. I. Jun, J. Oh, Y. J. Jeon and K. Kim, *Nature*, 2000, **404**, 982; (*b*) C.-D. Wu, A. Hu, L. Zhang and W. Lin, *J. Am. Chem. Soc.*, 2005, **127**, 8940; (*c*) C.-D. Wu and W. Lin, *Angew. Chem., Int. Ed.*, 2007, **46**, 1075.

4 (*a*) M. Dincă and J. R. Long, *Angew. Chem., Int. Ed.*, 2008, **47**, 6766; (*b*) M. Dincă, A. Dailly, Y. Liu, C. M. Brown, D. A. Neumann and J. R. Long, *J. Am. Chem. Soc.*, 2006, **128**, 16876; (*c*) M. Dincă, W. S. Han, Y. Liu, A. Dailly, C. M. Brown and J. R. Long, *Angew. Chem., Int. Ed.*, 2007, **46**, 1419; (*d*) S. Ma and H.-C. Zhou, *J. Am. Chem. Soc.*, 2006, **128**, 11734; (*e*) P. M. Forster, J. Eckert, B. D. Heiken, J. B. Parise, J. W. Yoon, S. H. Jhung, J.-S. Chang and A. K. Cheetham, *J. Am. Chem. Soc.*, 2006, **128**, 16846; (*f*) J. G. Vitillo, L. Regli, S. Chavan, G. Ricchiardi, G. Spoto, P. D. C. Dietzel, S. Bordiga and A. Zecchina, *J. Am. Chem. Soc.*, 2008, **130**, 8386.

5 (*a*) Y. K. Hwang, D.-Y. Hong, J.-S. Chang, S. H. Jhung, Y.-K. Seo, J. Kim, A. Vimont, M. Daturi, C. Serre and G. Férey, *Angew. Chem., Int. Ed.*, 2008, **47**, 4144; (*b*) A. Henschel, K. Gedrich, R. Kraehnert and S. Kaskel, *Chem. Commun.*, 2008, 4192; (*c*) S. Horike, M. Dinca, K. Tamaki and J. R. Long, *J. Am. Chem. Soc.*, 2008, **130**, 5854; (*d*) L. Alaerts, E. Seguin, H. Poelman, F. Thibault-Starzyk, P. A. Jacobs and D. E. De Vos, *Chem.–Eur. J.*, 2006, **12**, 7353; (*e*) K. Schlichte, T. Kratzke and S. Kaskel, *Microporous Mesoporous Mater.*, 2004, **73**, 81.

6 (*a*) M. Eddaoudi, J. Kim, N. Rosi, D. Vodak, J. Wachter, M. O'Keeffe and O. M. Yaghi, *Science*, 2002, **295**, 469; (*b*) S. A. Bourne, J. Lu, A. Mondal, B. Moulton and M. J. Zaworotko, *Angew. Chem., Int. Ed.*, 2001, **40**, 2111; (*c*) C. Serre, F. Millange, S. Surble and G. Férey, *Angew. Chem., Int. Ed.*, 2004, **43**, 6285.

7 (*a*) H. Asada, K. Hayashi, S. Negoro, M. Fujiwara and T. Matsushita, *Inorg. Chem. Commun.*, 2003, **6**, 193; (*b*) Y.-G. Li, L. Lecren, W. Wernsdorfer and R. Clerac, *Inorg. Chem. Commun.*, 2004, **7**, 1281; (*c*) X. S. Tan, J. Sun, C. H. Hu, D. G. Fu, D. F. Xiang, P. J. Zheng and W. X. Tang, *Inorg. Chim. Acta*, 1997, **257**, 203; (*d*) R. A. Coxall, A. Parkin, S. Parsons, A. A. Smith, G. A. Timco and R. E. P. Winpenny, *J. Solid State Chem.*, 2001, **159**, 321; (*e*) B. S. Luisi, Z. Ma and B. Moulton, *J. Chem. Crystallogr.*, 2007, **37**, 743.

8 *Materials Studio program*, version 4.3, Accelrys, San Diego, CA, 2008.

9 A. J. Arvai C. Nielsen *ADSC Quantum-210 ADX Program*, Area Detector System Corporation; Poway, CA, USA, 1983.

10 Z. Otwinowski; W. Minor in *Methods in Enzymology*, ed. Carter, Jr., C. W.; Sweet, R. M. Academic Press: New York, 1997, 276, part A, 307–326.

11 G. M. Sheldrick *SHELXTL–PLUS*, Crystal Structure Analysis Package; Bruker Analytical X-ray, Madison, WI, USA, 1997.

12 N. L. Rosi, J. Kim, M. Eddaoudi, B. Chen, M. O'Keeffe and O. M. Yaghi, *J. Am. Chem. Soc.*, 2005, **127**, 1504.

13 (*a*) R. Kitaura, K. Fujimoto, S.-i. Noro, M. Kondo and S. Kitagawa, *Angew. Chem., Int. Ed.*, 2002, **41**, 133; (*b*) G. Férey and C. Serre, *Chem. Soc. Rev.*, 2009, **38**, 1380.

14 X. Lin, I. Telepeni, A. J. Blake, A. Dailly, C. M. Brown, J. M. Simmons, M. Zoppi, G. S. Walker, K. M. Thomas, T. J. Mays, P. Hubberstey, N. R. Champness and M. Schröder, *J. Am. Chem. Soc.*, 2009, **131**, 2159.

15 (*a*) H. R. Moon, N. Kobayashi and M. P. Suh, *Inorg. Chem.*, 2006, **45**, 8672; (*b*) M. Xue, S. Ma, Z. Jin, R. M. Schaffino, G.-S. Zhu, E. B. Lobkovsky, S.-L. Qiu and B. Chen, *Inorg. Chem.*, 2008, **47**, 6825.

